Electronic Supplementary Material (ESI) for Journal of Materials Chemistry C.

Supporting Information

Suppression of Ion Migration in Lead-free Zero-dimensional Perovskite FA_3BiBr_6 Single Crystals for X-ray Detection

Kangyu Ji,[a] Wenjun Wang,*[b] Yuanbo Ma,[c] Zihan Wang,[c] Xuepeng Liu,[a] Jiajiu Ye,[c] Shu Zhang,*[d] Xu Pan, *[c] Songyuan Dai*[a]

[a]School of New Energy, North China Electric Power University, Beijing 102206, China. E-mail: sydai@ncepu.edu.cn

[b]Department of Microelectronics, Institute of Science, Hubei University of Technology, Wuhan 430068, China

[c]Chinese Acad Sci, Inst Solid State Phys, Hefei Inst Phys Sci, Hefei 230031, Peoples R China

[d]Qingdao Institute of Bioenergy and Bioprocess Technology, Chinese Academy of Sciences, Qingdao 266101 P.R. China

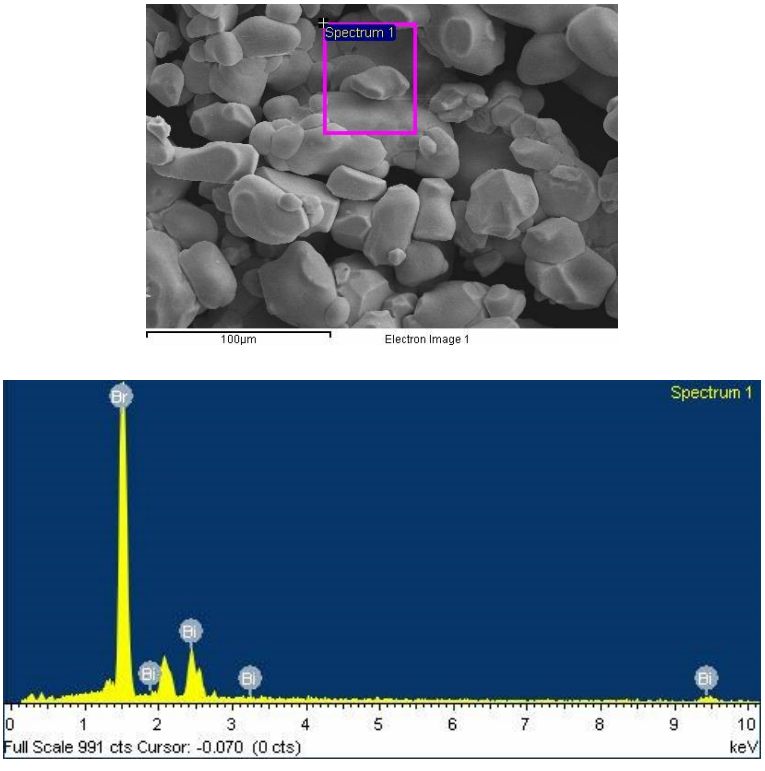

Figure S1. Single crystal ground into powder detection EDS.

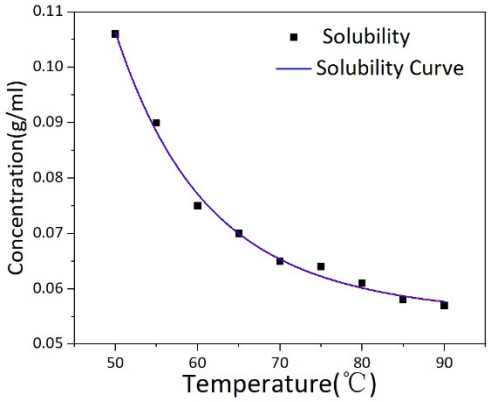

Figure S2. The solubility curve of FA_3BiBr_6 SC powder in GBL solvent.

Figure S3. FA_3BiBr_6 crystals growth at 75 °C and crystals after vacuum drying.

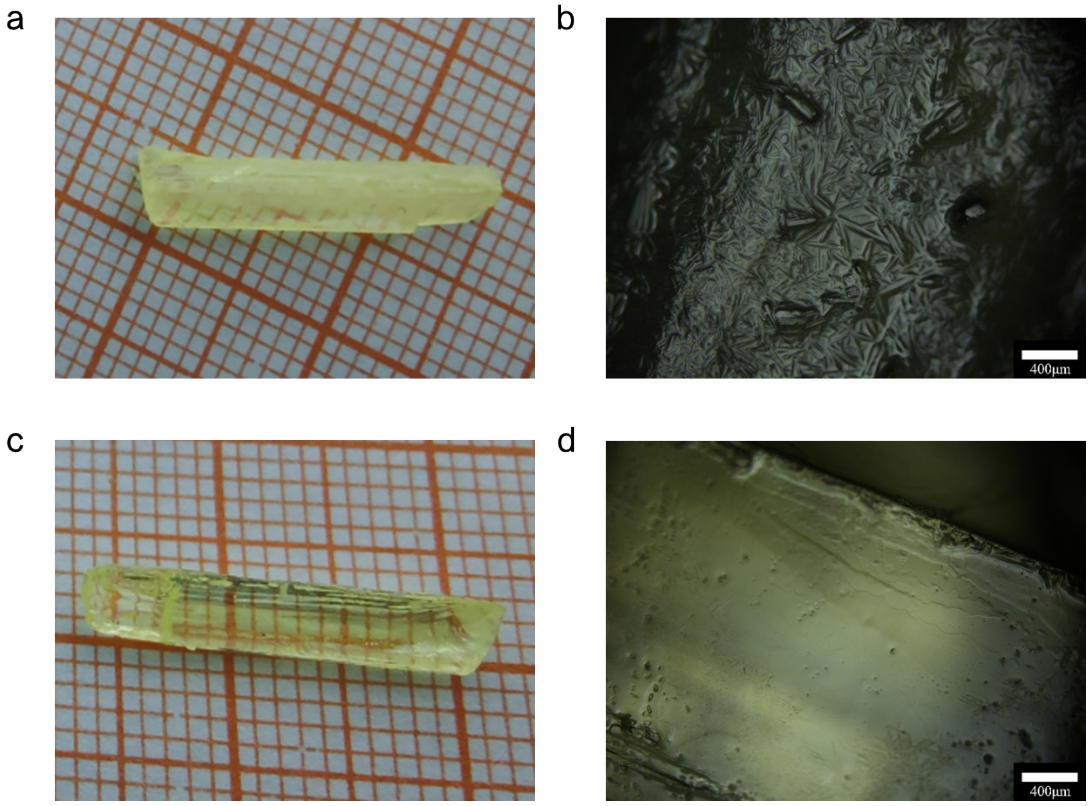

Figure S4. (a) Photograph of FA_3BiBr_6 PSCs dried directly without washing and (b) 80X magnification of the surface of PSCs under a microscope. (c) Photograph of FA_3BiBr_6 PSCs dried after cleaning with GBL and (d) 80X magnification of the surface of PSCs under microscope

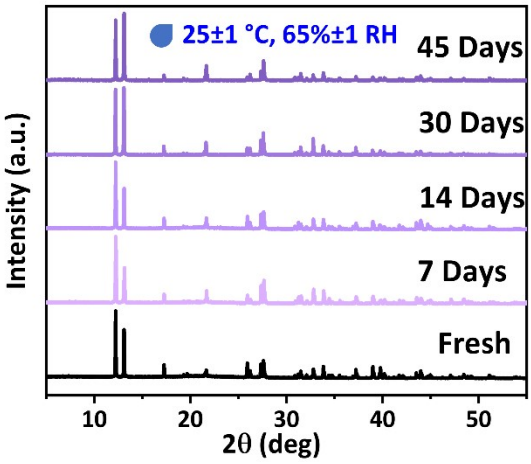

Figure S5. PXRD pattern of FA_3BiBr_6 placed in 65% humidity and dry environment for 45 days.

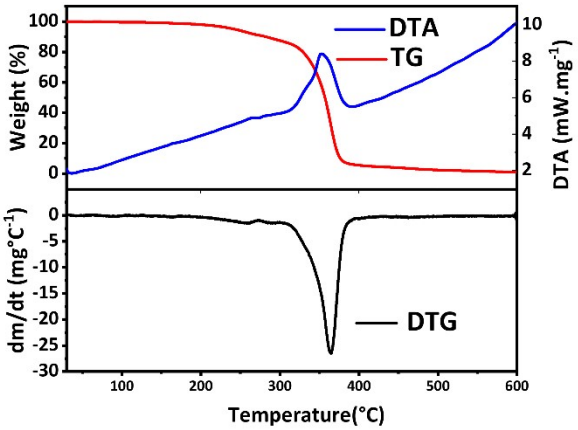

Figure S6. TG, DTG and DTA data for FA_3BiBr_6 (TG = thermogravimetric analysis (mass loss vs. temperature) plot, DTG = thermogravimetric analysis first order derivative, DTA = free carrier stat).

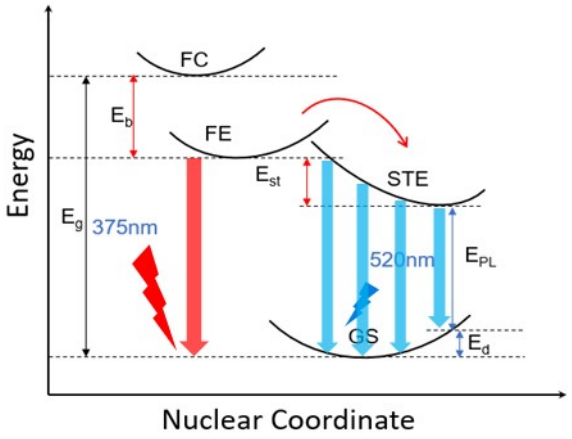

Figure S7. Schematic of the energy level structure of STE (FC = free carrier state, FE = free exciton state, STE = self-trapped exciton state, GS = ground state).

Figure S7 illustrates the emission process of the two types of excitons. The excitons are initially excited to the conduction band and subsequently relax at the edge of the conduction band. At this point, the excitons are in the free exciton state (FE). When the excitation energy surpasses E_g of 2.75 eV in FA_3BiBr_6, the free exciton pairs consisting of holes and electrons overcome the binding energy (E_b) restriction of excitons. The energy levels of these carriers are situated in the free-carrier state (FC). The emission of free excitons (FEs) involves a direct transition from the free exciton state to the ground state (GS), as indicated by the red arrow in Figure 4c. However, the presence of electron-phonon coupling leads to the loss of energy by high-level FEs, causing their transformation into low-level STEs. This energy loss is referred to as self-trapping energy (E_{st}).[1] Additionally, the energy of the ground state is influenced by lattice deformation, resulting in an increase known as lattice deformation energy (E_d). Emission of STEs from different states of STE to different states of GS was affected by E_{st} and E_d, as illustrated by the blue arrows in Figure S7. This phenomenon also accounts for the broad-spectrum emission of STEs and the

large Stokes shift observed in FA_3BiBr_6. The emission energy (E_{PL}) can be calculated using the equation $E_{PL} = E_g - E_b - E_{st} - E_d$.

Table S1. EDS test report

Element	App	Intensity	Weight%	Weight%	Atomic%
	Conc.	Corrn.		Sigma	
Br L	12.87	0.9312	69.86	1.02	85.84
Bi M	3.71	0.6229	30.14	1.02	14.16
Totals			100		

Table S2. Crystal data and structure refinement for FA_3BiBr_6

Empirical formula	**$C_3H_{15}BiBr_6N_6$**
Formula weight	823.65
Temperature/K	300.00
Crystal system	tetragonal
Space group	$P4_2/m$
a/Å	10.3603(6)
b/Å	10.3603(6)
c/Å	9.0922(6)
α/°	90
β/°	90
γ/°	90
Volume/Å^3	975.92(13)
Z	2
ρ_{calc}g/cm^3	2.803
μ/mm^{-1}	21.305
F(000)	736.0
Crystal size/mm^3	0.26 × 0.23 × 0.17
Radiation	MoKα (λ = 0.71073)
2θ range for data collection/°	5.56 ~ 61.054
Index ranges	$-13 \leq h \leq 14$, $-14 \leq k \leq 14$, $-12 \leq l \leq 12$
Reflections collected	27474
Independent reflections	1577 [R_{int} = 0.1223, R_{sigma} = 0.0509]
Data/restraints/parameters	1577/64/76
Goodness-of-fit on F^2	1.035
Final R indexes [I ≥ 2σ (I)]	R_1 = 0.0451, wR_2 = 0.0980
Final R indexes [all data]	R_1 = 0.0945, wR_2 = 0.1152
Largest diff. peak/hole / e Å^{-3}	0.75/-0.93

Table S3. Selected bond lengths for FA_3BiBr_6

Atom	Atom	Length/Å	Atom	Atom	Length/Å
Bi1	Br1	2.8387(12)	Bi1	Br2[1]	2.8517(8)
Bi1	Br1[1]	2.8388(12)	N1	C1	1.386(10)
Bi1	Br2[2]	2.8517(8)	N2	C1	1.334(10)
Bi1	Br2[3]	2.8517(8)	N3	C2	1.4000(11)
Bi1	Br2	2.8517(8)	N4	C2	1.351(10)

Table S4. Selected bond angles (deg) for FA_3BiBr_6

Atom	Atom	Atom	Angle/°	Atom	Atom	Atom	Angle/°
Br1	Bi1	$Br1^1$	180.0	$Br2^3$	Bi1	$Br2^2$	180.00(3)
Br1	Bi1	$Br2^2$	89.14(3)	$Br2^2$	Bi1	Br2	89.23(5)
$Br1^1$	Bi1	Br2	89.14(3)	$Br2^1$	Bi1	$Br2^2$	90.77(5)
$Br1^1$	Bi1	$Br2^3$	89.14(3)	$Br2^3$	Bi1	Br2	90.77(5)
$Br1^1$	Bi1	$Br2^1$	90.86(3)	$Br2^1$	Bi1	Br2	180.0
Br1	Bi1	Br2	90.86(3)	$Br2^1$	Bi1	$Br2^3$	89.23(5)
Br1	Bi1	$Br2^3$	90.86(3)	N2	C1	N1	119(2)

Table S5. The dark current drift values of perovskite material

Materials	Dimension	Applied Electric Field ($V\ cm^{-1}$)	Dark Current Drift ($nA\ cm^{-1}\ s^{-1}\ V^{-1}$)	Device Type	Reference
$MAPbI_3$ single crystal	3D	100	1.4×10^{-4}	vertical	2
$CsPbBr_3$ single crystal	3D	2000	1.9×10^{-4}	vertical	3
$MAPbBr_3$ single crystal	3D	20	1.2×10^{-3}	vertical	4
$MAPbBr_{3-n}Cl_n$ /$CsPbBr_3$ Heterojunction	3D	1250	3.92×10^{-4}	vertical	5
BiOBr passivated $Cs_2AgBiBr_6$ film	3D	5000	7.4×10^{-5}	vertical	6
BA_2PbI_4 /$MAPbI_3$	2D/3D	125	4.84×10^{-5}	vertical	7
$(F\text{-}PEA)_2PbI_4$	2D	1333	4.9×10^{-8}	vertical	8
$(PEA)_2Pbl_4$ single crystal	2D	4545	1.9×10^{-7}	planar	9
$(PEA)_2PbBr_4$ single crystal	2D	4545	6.2×10^{-6}	planar	
δ-$FAPbI_3$	1D	100	3.43×10^{-7}	vertical	10
$MA_3Bi_2I_9$	0D	4545	5×10^{-10}	planar	9
Cs_4PbBr_6	0D	6667	5.6×10^{-11}	planar	11
$Cs_3Bi_2I_9$	0D	100	1.67×10^{-8}	planar	12
FA_3BiBr_6	**0D**	**200**	**3.73×10^{-7}**	**vertical**	**This work**

Table S6. Perovskite Br-Br spacing in different dimensions

Component	Dimension	Br-Br Maximum distance（Å）	Br-Br Minimum distance （Å）	Reference
$FAPbBr_3$	3D	4.2404	4.2404	[13]
$FA_3Bi_2Br_9$	2D	5.938	3.889	[14]
FA_3BiBr_6	0D	6.432	4.0533	**This work**

Table S7. The activation energy values of perovskite materials

Materials	Dimension	Activation Energy (eV)	Device Type	Reference
$MAPbBr_3$	3D	0.062	SC	[15]
$CsPbBr_3$	3D	0.228	SC	[16]
$MAPbBr_3$	3D	0.127	SC	[17]
$MAPbBr_3$	3D	0.25	film	[18]
$Cs_2AgBiBr_3$	3D	0.348	SC	[17]
$Cs_3Bi_2Br_9$	2D	0.15	film	[19]
$[(CH_3)_2NH_2]_2PdBr_4$	2D	0.27	SC	[20]
$BA_2MA_2Pb_3Br_{10}$	2D	0.052	SC	[21]
$PEA_2Pb(Br_{0.5}I_{0.5})_4$	2D	0.226	film	
$PEA_2MA_5Pb_6(Br_{0.5}I_{0.5})_{19}$	2D	0.213	film	[22]
$PEA_2MA_9Pb_{10}(Br_{0.5}I_{0.5})_{31}$	2D	0.17	film	
δ-$FAPbI_3$	1D	0.52	wafer	[10]
Cs_4PbI_6 single crystal	0D	0.32	vertical	[23]
$MA_3Bi_2I_9$ single crystal	0D	0.46 (in-plane) 0.31 (out-of-plane)	vertical	[24]
FA_3BiBr_6	**0D**	**0.54**	**SC**	**This work**

SC=single crystal

References

1. S. Li, J. Luo, J. Liu and J. Tang, *J Phys Chem Lett*, 2019, **10**, 1999-2007.
2. S. Yakunin, D. N. Dirin, Y. Shynkarenko, V. Morad, I. Cherniukh, O. Nazarenko, D. Kreil, T. Nauser and M. V. Kovalenko, *Nat. Photonics*, 2016, **10**, 585-589.
3. Y. H. He, L. Matei, H. J. Jung, K. M. McCall, M. Chen, C. C. Stoumpos, Z. F. Liu, J. A. Peters, D. Y. Chung, B. W. Wessels, M. R. Wasielewski, V. P. Dravid, A. Burger and M. G. Kanatzidis, *Nat. Commun.*, 2018, **9**.
4. W. Wei, Y. Zhang, Q. Xu, H. Wei, Y. Fang, Q. Wang, Y. Deng, T. Li, A. Gruverman, L. Cao and J. Huang, *Nat. Photonics*, 2017, **11**, 315-321.
5. F. C. Cui, P. Zhang, L. Z. Zhang, Y. Q. Hua, X. Sun, X. Li, G. D. Zhang and X. T. Tao, *Chem. Mater.*, 2022, DOI: 10.1021/acs.chemmater.2c02266.
6. B. Yang, W. C. Pan, H. D. Wu, G. D. Niu, J. H. Yuan, K. H. Xue, L. X. Yin, X. Y. Du, X. S. Miao, X. Q. Yang, Q. G. Xie and J. Tang, *Nat. Commun.*, 2019, **10**.
7. Y. R. Xiao, C. Z. Xue, X. Wang, Y. C. Liu, Z. Yang and S. Z. Liu, *ACS Appl. Mater. Interfaces*, 2022, **14**, 54867-54875.
8. H. Y. Li, J. M. Song, W. T. Pan, D. R. Xu, W. A. Zhu, H. T. Wei and B. Yang, *Adv. Mater.*, 2020, **32**.
9. Y. Liu, Z. Xu, Z. Yang, Y. Zhang, J. Cui, Y. He, H. Ye, K. Zhao, H. Sun, R. Lu, M. Liu, M. G. Kanatzidis and S. Liu, *Matter*, 2020, **3**, 180-196.
10. Z. H. Wang, S. J. Tie, H. Zhang, C. M. Wan, Z. Liang, H. F. Xu, X. J. Zheng, W. H. Zhang, D. Aldakov, P. Reiss, J. J. Ye and X. Pan, *ACS Nano*, 2023, **17**, 13638-13647.
11. H. Y. Chen, B. Y. An, G. Q. Peng, S. Wang, Z. H. Li, J. Sun, W. Lan, J. J. Fu, H. X. Wang, L. M. Ding and Z. W. Jin, *Advanced Optical Materials*, 2023, **11**.
12. L. J. Li, G. Ye, T. Y. Luo, X. Y. Chen, G. J. Zhang, H. Wu, L. Yang, W. F. Zhang and H. X. Chang, *J. Phys. Chem. C*, 2022, **126**, 3646-3652.
13. C. Li, E. J. Juarez-Perez and A. Mayoral, *Chem. Commun. (Camb.)*, 2022, **58**, 12164-12167.
14. R. Bhowal, A. A. Balaraman, M. Ghosh, S. Dutta, K. K. Dey and D. Chopra, *J. Am. Chem. Soc.*, 2021, **143**, 1024-1037.
15. V. K. Sharma, R. Mukhopadhyay, A. Mohanty, M. Tyagi, J. P. Embs and D. D. Sarma, *Journal of Physical Chemistry Letters*, 2020, **11**, 9669-9679.
16. M. L. Xia, J. H. Yuan, G. D. Niu, X. Y. Du, L. X. Yin, W. C. Pan, J. J. Luo, Z. G. Li, H. T. Zhao, K. H. Xue, X. S. Miao and J. Tang, *Adv. Funct. Mater.*, 2020, **30**.
17. W. Pan, H. Wu, J. Luo, Z. Deng, C. Ge, C. Chen, X. Jiang, W.-J. Yin, G. Niu, L. Zhu, L. Yin, Y. Zhou, Q. Xie, X. Ke, M. Sui and J. Tang, *Nat. Photonics*, 2017, **11**, 726-732.
18. L. McGovern, M. H. Futscher, L. A. Muscarella and B. Ehrler, *Journal of Physical Chemistry Letters*, 2020, **11**, 7127-7132.
19. J. H. Xu, J. P. Xu, S. B. Shi, W. H. Bian, J. Chen, Q. L. Zhu, Z. Wang, L. A. Kong, X. S. Zhang and L. Li, *Journal of Physical Chemistry Letters*, 2023, **14**, 5318-5327.
20. K. Trabelsi, N. Drissi, F. Hajlaoui, M. Zighrioui, A. Rhaiem, N. Audebrand, T. Roisnel and K. Karim, *Rsc Advances*, 2023, **13**, 23348-23358.

21. H. H. Tsai, D. Ghosh, E. Kinigstein, B. Dryzhakov, H. Driscoll, M. Owczarek, B. Hu, X. Y. Zhang, S. Tretiak and W. Y. Nie, *Nano Lett.*, 2023, **23**, 429-436.
22. J. Cho, P. S. Mathew, J. T. DuBose and P. V. Kamat, *Adv. Mater.*, 2021, **33**.
23. Q. Xu, C. Li, J. Nie, Y. Guo, X. Wang, B. H. Zhang and X. P. Ouyang, *Journal of Physical Chemistry Letters*, 2021, **12**, 287-293.
24. X. J. Zheng, W. Zhao, P. Wang, H. R. Tan, M. I. Saidaminov, S. J. Tie, L. G. Chen, Y. F. Peng, J. D. Long and W. H. Zhang, *Journal of Energy Chemistry*, 2020, **49**, 299-306.